

## A Hybrid Approach Based on Numerical, Statistical and Intelligent Techniques for Optimization of Tube Drawing Process to Produce Squared Section from Round Tube

M. Ghasempour-Mouziraji<sup>1\*</sup>, M. Hosseinzadeh<sup>2</sup>, M. Bakhshi-Jooybari<sup>3</sup> and J. Maktoubian

<sup>1</sup>Department of engineering, Islamic Azad university of Sari, Sari, Iran.

<sup>2</sup>Department of engineering, Ayatollah Amoli Branch, Islamic Azad university, Amol, Iran.

<sup>3</sup>Department of Mechanical engineering, Babol Noshirvani University of Technology, Iran.

<sup>4</sup>International School of Information Management (ISIM), University of Mysore, Mysore, India.

**Abstract:** In tube drawing process, there is a bunch of parameters playing key roles in the process performance. Thus finding the optimized parameters is a controversial issue. The current study aimed to produce a squared section of round tube by tube sinking process. Finite element method (FEM) was used to simulate the process. Then, to find a meaningful kinship between process input and output parameters the developed FE model was associated with the design of an experiment based on response surface methodology (RSM). The sufficiency of each model was checked by analyzing the variances. Further, the SA (simulated annealing) was associated with RSM models to find the optimal solution regarding maximum thickness distributions and minimum force and dimensional error. Hereafter, for performing accurate optimization, principal component analysis was used to find the appropriate weight factor of each response. The obtained results were in right congruence with those derived from the simulation and confirmatory experiment.

**Keywords:** Tube sinking, square sections, Multi-objective optimization.

### 1. Introduction

Polygonal tubes are widely used in various engineering and industrial applications to produce lightweight structures [1]. There are four main methods used to produce tubes, namely tube sinking, tube drawing with fixed mandrel, tube drawing with floating mandrel and tube drawing with movable mandrel. In tube sinking process, the tubes are pulled out through the die with no underlying support, and the tube's diameter decreases and its thickness remains constant but it might increase on some occasions. Having low surface quality is the main disadvantage of this method. Bayoumi et al [2] produced polygonal tubes by using rollers which are shapely-located. The roller's radius, thickness, section shape and friction coefficient were investigated to find the drawing force in this process.

In tube drawing with fixed mandrel, the primary tube is drawn after being placed on the mandrel. Thickness and diameters decrease but both inner and outer surfaces are good in quality. Mandrels could have different shapes due the desired shape of the tube and also they play key roles in the dimensional accuracy of the produced tubes. The high rate of friction between the tubes and mandrel leads the low accuracy of the produced tubes due to the corrosion between them. As previously mentioned, fixed mandrels are associated with some problems but tube drawing with floating mandrel has tackled this task. The cone-shaped mandrel is constant in the deformation zone which has contact with the inner surface of the tube, and the balance between the compressive and frictional forces in this location remains constant.

In tube drawing with movable section, the mandrel is located in the primary tube and passes through the die with the tube. The goals of this process are to decrease the thickness and increase the length of the tube. Numerous researches in shaping round tubes have been carried out by many researchers. The production of rectangular tubes by using hydroforming expansion has been compared with combined hydraulic expansion and hydroforming [3]. Manabe and Amino have already investigated on circular tubes into square tubes [4]. Kridli et al [5] carried out the die geometry and material property in producing square tubes by using hydroforming considering two-dimensional plane strain FE code. Experimental and numerical investigations of tube drawing with various thicknesses were conducted by Bihamta et al [6]. Leu et al [7] designed a die which was able to prevent fracture by using damage criteria. Boton et al [8] developed a model for tube drawing with fixed mandrel by using numerical and mathematical formulae. MSC.SUPERFORM was used in this research, then the numerical and experimental results were compared. Finally, they found that, 7-10 die half angle was the most suitable angle for drawing, and that condition plays a key role in this process. Karenzis et al [9] developed a model for cold tubes which are sensitive to thermal variation. Residual stress, tension force, and the efficiency of the process were investigated via ABAQUS. Production of thin tubes which are used in medical applications was studied by Yushida et al [10]. They used titanium material and MARC software in their research. They have found that tube sinking has the highest thickness increase among different methods of tube drawing. Also, various studies have been carried out to optimize the manufacturing process by using statistical methods in machining [11, 12], welding [13, 14], metal forming [15, 16], coating [15, 16] and etc. Therefore, the method has found applicability to the problems and could be applied in modeling and optimization of tube drawing process. Many researches have employed RSM to optimize different processes, such as tube drawing process which was used to produce square-shaped tubes by M. Hosseinzadeh et al. [17]. They optimized tube drawing process parameters such as entrance velocity, bearing length, friction coefficient, and die angle by using FE simulation and experimental test. The central composite design matrix was used for achieving optimum parameters. M. Salehi et al [18] utilized DOE (design of experiment), RSM and artificial bee ant colony algorithm to optimize the parameters of rectangular tubes. They investigated the effects of the parameters on geometrical error, thickness distribution and drawing force. Mirshaban Jafari et al [19] optimized the spring back phenomenon in deep drawing process by using ANFIS to attain the least spring back.

Square tubes which are produced by different methods such as hydroforming are really expensive and the process should be controlled accurately to prevent leakage of oil and fracture. Preparing adequate pressure for this process, the tubes maintained their circular shape until the end of the process; however, wrinkling and buckling are other challenges that can be mentioned here. In addition, rolling could be a useful method but its disadvantages outweigh its advantages. Take, for example, flat-shaped rollers. They can produce square tubes but positioning the rollers is the main challenge in this process. The harder the material, the more the vibration and the more the power which will be used. Furthermore, the rollers' wear is another problem in this process. Eventually, the tube sinking process has been introduced to address this problem. Its advantages are its low cost, flexibility to produce different sections, higher speed than the above-mentioned processes and capability to fabricate micro and complex shapes from round tubes. The geometry and drawing parameter of the final products have crucial roles in the fabrication of the square section, and if the parameters are controlled simultaneously, the thickness distribution and dimensional accuracy are augmented and the drawing force is swelled. In the current research, some dies have been designed via CATIA and manufactured. The main goal of this study is to discover the best combination of process parameters to reach the lowest drawing force and dimensional accuracy as well as the highest thickness distribution in round to square pure copper tube sinking. Finite element model of the process is developed via ABAQUS/EXPLICIT prior to running experimental tests. Response surface methodology (RSM), particularly face-centered central composite design, is used to reduce the computing time based on the

results which have been achieved by FE simulation. One key factor that should be considered in multi-objective optimization is finding adequate weight of each response that has been achieved in this research by PCA (principal component analysis). Simulated annealing algorithm is used to integrate the RSM model and achieve weight factor by using singular objective function. It is worth notifying that singular objective function is derived from weighted function for each factor (force, MSE, thickness) to reach a sole and target function in order to proceed the optimization. Lastly, once the optimal results found, the data are validated through experimental and simulation results. The current study is classified into seven steps that can be seen in this section.

1. Finding the mechanical properties of the material running FE simulation
2. Validating the FE result by performing experimental tests (choosing the same condition in the simulation and experiments)
3. Creating a statistic model of each response with RSM
4. Using ANOVA to check the sufficiency of the model
5. Obtaining weight factor of each response through PCA and developing a singular objective function
6. Utilizing simulated annealing to optimize objective function and draw out the results which have been optimized
7. Using FE model and experimental tests to confirm the achieved results

## 2. Experimental Steps

Pure copper tubes have been utilized for running the experimental tests and FE model. Also, tension test has been used based on ASTM-A370 standard to find the mechanical properties of copper tubes. The sample was considered as a deformable pure copper tube with the stress-strain relationship of  $\sigma=402\epsilon^{0.32}$  MPa where 402 MPa is strength coefficient and 0.32 is strain hardening exponent which was determined experimentally using tensile test data. It is worth notifying that the tube's thickness is 0.75 mm and the inner diameters is 11.2. Table 1 elucidates the mechanical properties of the tubes.

Table 1. Mechanical properties of pure copper.

Density (kg/m <sup>3</sup> )	Yield strength (MPa)	Ultimate tensile strength (MPa)	Young modulus (GPa)	Poisson coefficient
8900	180	270	110	0.343

A hand-made drawing machine with 3KW capacity has been used to run the experimental tests. The drawing machine was equipped with an inverter to control the velocity which should be used in this process. To perform the drawing process, the tube is drawn through the die with a series of chains.

Figure 1a illustrates the drawing machine with the dies and Fig. 1c depicts various parameters of the process. It is worth notifying that, the length of the sides in the dies is 9 mm.

One of the most important and challenging issues in tube sinking process to produce square section is corner fillets which deteriorate dimensional accuracy. It can be mentioned that there is difference between the produced tubes and the ones anticipated (Fig. 2). In addition, another parameter which plays a key role in shape and dimensional accuracy is springback. The dimensional accuracy has been measured by VMM (video measurement machine) and MSE (mean square error) equation which is shown here

$$MSE = \frac{1}{N} \sum_{i=1}^n (d_e - d_o)^2 \quad (1)$$

In MSE equation,  $N$ ,  $d_e$  and  $d_o$  are the numbers of measurement points on drawn section, anticipated and achieved dimensions, respectively. The thickness distribution was measured in 30 points by digital micro meter in two paths which one is linear and the other is peripheral.

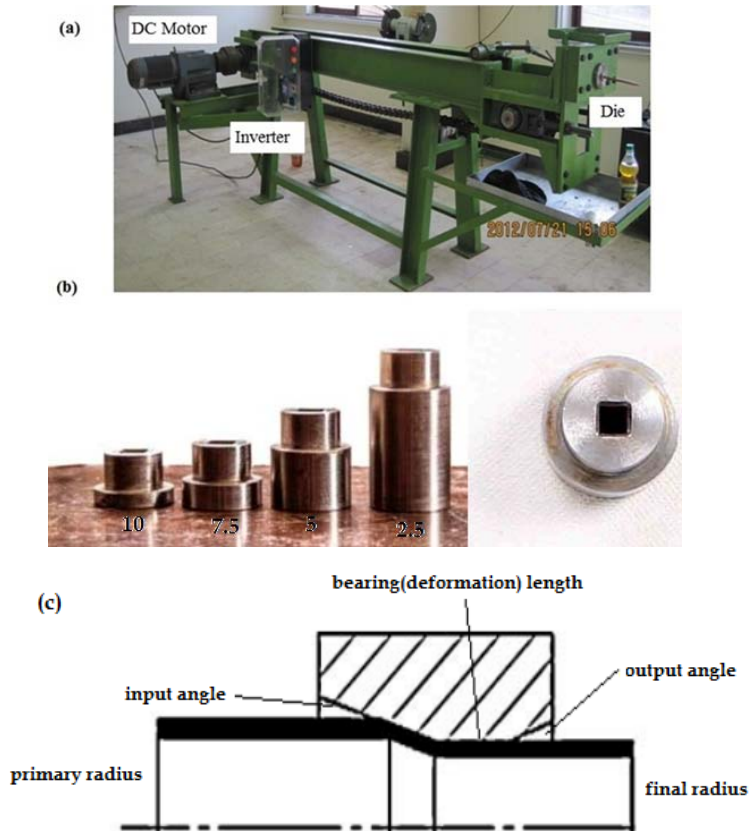


Fig. 1. Experimental setup (a) details of the drawing machine (b) Square dies with different input angles and various parameters of the process.

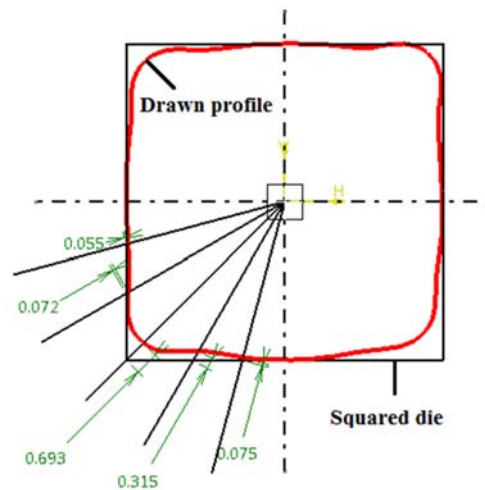


Fig. 2. calculation of MSE and its schematic view

### 3. Finite Element Simulation

3D FE model based on ABAQUS/EXPLICIT 6/14 code has been developed for simulating the tube sinking which is shown in Fig. 3. The dies were considered as a rigid body by R3D4 element type

because it has no conspicuous deformation compared with the tube that has been modeled as a deformable body by C3D8R. Different friction models can be used in simulation via ABAQUS, but in the current study surface to surface model was utilized. The velocity and symmetry boundary conditions have been used to model the movement of the tube and fix the die. Three friction coefficients were used in simulation according to different lubricants, SAE 10, sunflower oil and grease which were considered 0.1, 0.2 and 0.3, respectively. Tension test has been employed to achieve the pure copper property which has 99.9 purity. One of the most controversial issues in tube drawing process is the thermal effect that should be considered but in this research, it has been ignored due to the drawn tube's temperature. Drawn tube's temperature was measured by a thermocouple and the highest temperature was 70°C which due to the melting temperature of the pure copper, it was about 7% [1,2,6].

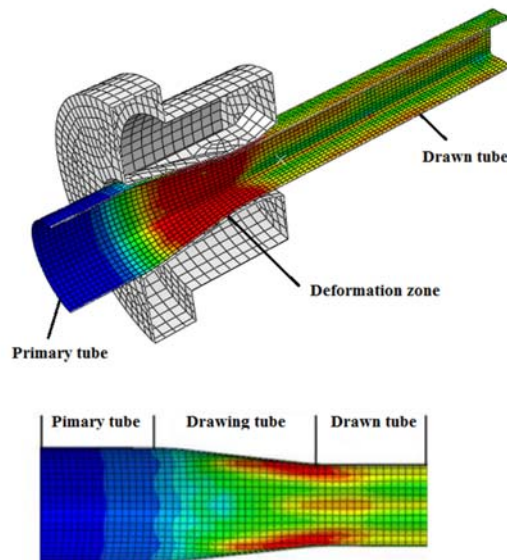


Fig. 3. Finite element modelling of tube drawing and its definition.

### 3.1. FE Model's validation

FE model of the process has been validated with experimental results, namely dimensional accuracy and thickness distribution. As can be seen in Fig. 4, there is adequate correlation between the experimental and numerical results.

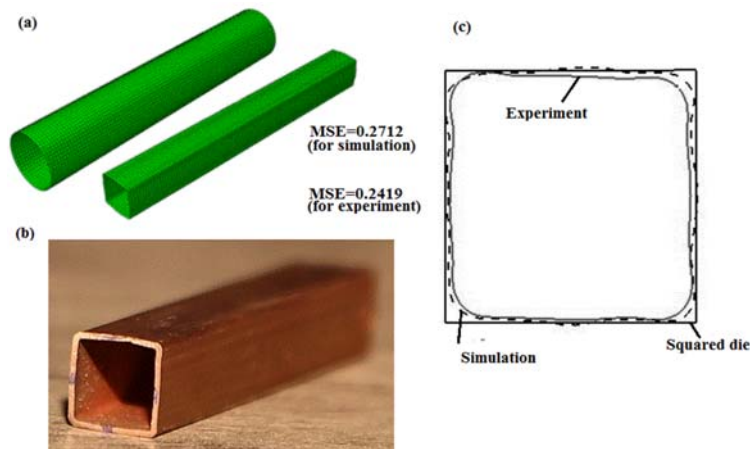


Fig. 4. Comparison of the experimental and numerical results (a) drawn tube simulation (b) drawn tube from experiment (c) section of drawn tube.

The accuracy of FE model has been analyzed with thickness distribution in two paths, linear and peripheral. Figure 5 depicts both linear and peripheral paths and it can be found that there is good correlation between the experimental and FE results.

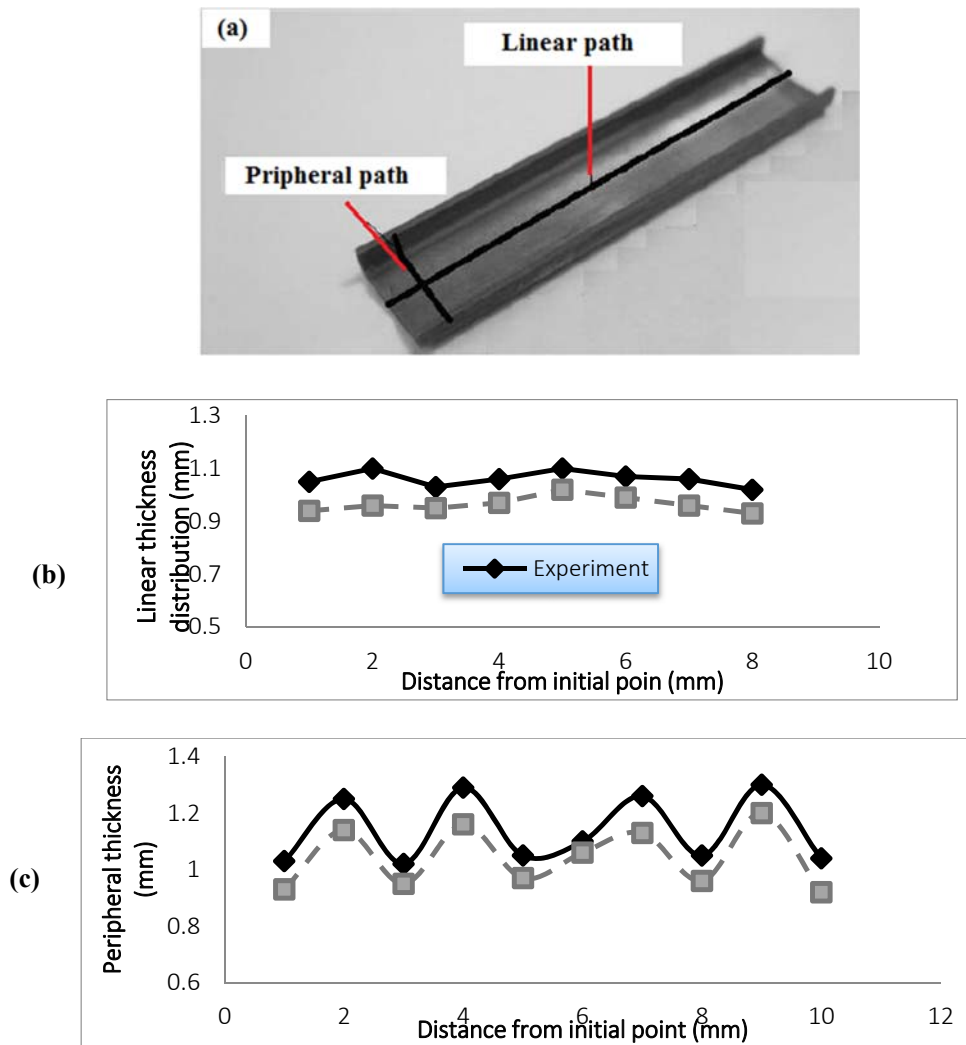


Fig. 5. Thickness distribution along two directions.

#### 4. Designing the Experiment and Developing RSM Models

##### 4.1. Construction design matrix

In the previous section, the accuracy of FE results was validated and it could be useful to anticipate the characteristic which is one of the main goals of the current research. However, it takes much more time, several hours, to run all simulation. RSM is a more suitable method for anticipation and has been used in this research to find the correlation between tube sinking parameters and process responses (Drawing force, MSE, and thickness distribution). Data have been collected based on simulations and design of experiment (DOE). Input parameters are die half angle, friction coefficient and bearing length and have been considered in three levels which are shown in Table 2. 81 experiments are required to run full factorial design which is calculated according to  $N=L^m$  formula that N, L and m are the numbers of possible design, level of each factor and number of factor, respectively. Five factors-three levels face-centered central composite design has been employed to reach additional reduction. To achieve this goal, 25 are required to gather the data for

running RSM. For testing the adequacy of the model, analysis of variance (ANOVA) has been used. Design matrix and achieved values have been depicted in Table 3.

Table 2. Process factors and their levels.

Factors	Symbol	Unit	Level 1	Level 2	Level 3
Die angle	$\alpha$	deg	2.5	5	7.5
Deformation length	$L$	mm	2	4	6
friction coefficient	$\mu$	-	0.1	0.2	0.3
Drawing velocity	$V$	mm/min	5	7.5	10

Table 3. Face centered central composite design matrix and obtained values of responses.

No	$\alpha$ (deg)	L (mm)	$\mu$	V (mm/min)	Force (N)	linear thickness (mm)	peripheral thickness (mm)	MSE
1	2.5	2	0.1	5	8888.95	0.9465	1.2750	0.3812
2	7.5	2	0.1	5	5211.44	0.9434	1.2795	0.3564
3	2.5	6	0.1	5	8533.22	1.2346	0.9500	0.3785
4	7.5	6	0.1	5	4959.68	0.9458	1.2859	0.4941
5	2.5	2	0.3	5	21727.9	0.9458	1.2535	0.1726
6	7.5	2	0.3	5	10567.3	0.9324	1.2779	0.3092
7	2.5	6	0.3	5	20778.3	0.9493	1.2304	0.1734
8	7.5	6	0.3	5	9457	0.9539	1.2853	0.3739
9	2.5	2	0.1	10	8910.56	0.9460	1.2788	0.3991
10	7.5	2	0.1	10	5228.94	0.9452	1.2691	0.4639
11	2.5	6	0.1	10	8497.99	0.9500	1.2363	0.4091
12	7.5	6	0.1	10	4964	0.9536	1.2901	0.5021
13	2.5	2	0.3	10	21852.1	0.9471	1.2612	0.1504
14	7.5	2	0.3	10	10551.7	0.9377	1.2748	0.3103
15	2.5	6	0.3	10	20700	0.9502	1.2333	0.1746
16	7.5	6	0.3	10	9391	0.9555	1.2897	0.3746
17	2.5	4	0.2	7.5	14981.6	0.9490	1.2328	0.2365
18	7.5	4	0.2	7.5	7595.85	0.9496	1.2692	0.4123
19	5	2	0.2	7.5	9281.6	0.9414	1.2632	0.3832
20	5	6	0.2	7.5	9270.14	0.9334	1.2774	0.3900
21	5	4	0.1	7.5	5951	1.2804	0.9391	0.4836
22	5	4	0.3	7.5	12639.2	1.2821	0.9395	0.2712
23	5	4	0.2	5	9216.66	1.2924	0.9436	0.3873
24	5	4	0.2	10	9256.47	1.2745	0.9499	0.3897
25	5	4	0.2	7.5	9250.72	1.2726	0.9442	0.3915

#### 4.2. Development of RSM model for each response

As previously-mentioned, RSM has been used to discover the correlation between the parameters. When the effects of the parameters were studied, then the mathematical model, second-order polynomial was developed which is shown in Eq. (2).

$$Y = b_0 + \sum_{i=1}^k b_i X_{iu} + \sum_{i=1}^k b_{ii} X_{iu}^2 + \sum_{i=1}^k \sum_{j=1}^k b_{ij} X_{iu} X_{ju} \quad (2)$$

In Eq. (2), Y is response (peripheral thickness and linear thickness distribution, MSE and drawing force) and coefficient, variable, experiment number, factor number, higher order term of variable and interaction terms are shown by  $b_0$ ,  $b_i$ ,  $b_{ii}$  and  $b_{ij}$ ,  $X_{iu}$  ( $V$ ,  $L$ ,  $\alpha$ , and  $\mu$ ),  $u(1-15)$ ,  $k(1-4)$ ,  $X_{iu}^2$  and  $X_{iu}$ ,  $X_{ju}$ , respectively.

##### 4.2.1. RSM model of responses

By using design expert and the data which have been achieved from Table 3, effects of parameters have been calculated by considering Eq. (2) constants. Equation (3-6) depict the mathematical relationship of responses.

Drawing force's equation

$$\begin{aligned}
 \text{Force} = & 8075.5 - 3178.33\alpha + 55.44L + 83860.05\mu + 111.31V + 1.028\alpha L \\
 & - 765.16\alpha\mu - 0.92\alpha V - 964.9L\mu - 4.03LV - 10.97\mu V + 322.47\alpha^2 \\
 & + 0.649L^2 + 2182.7\mu^2 - 5.873V^2
 \end{aligned}
 \tag{3}$$

MSE's equation

$$\begin{aligned}
 \text{MSE} = & 0.39 + 0.062\alpha + 0.019L - 0.087\mu + 8.17 \times 10^{-3}V + 0.017\alpha L \\
 & + 0.028\alpha\mu + 5.61 \times 10^{-3}\alpha V - 1.82 \times 10^{-3}L\mu - 3.98 \times 10^{-3}LV \\
 & - 0.011\mu V - 0.057\alpha^2 + 5.36 \times 10^{-3}L^2 - 3.83 \times 10^{-3}\mu^2 + 7.26 \times 10^{-3}V^2
 \end{aligned}
 \tag{4}$$

Thickness distribution's equation

$$\begin{aligned}
 \text{Linear} = & 0.808 + 0.338\alpha + 0.551L - 4.78\mu - 0.27V - 3.1 \times 10^{-3}\alpha L \\
 & + 0.06\alpha\mu + 2.99 \times 10^{-3}\alpha V - 0.08L\mu - 3.52 \times 10^{-3}LV + 0.07\mu V \\
 & - 0.03\alpha^2 + -0.06L^2 + 10.15\mu^2 + 0.01V^2
 \end{aligned}
 \tag{5}$$

$$\begin{aligned}
 \text{Peripheral} = & 1.53 - 0.32\alpha - 0.55L + 4.41\mu + 0.23V + 5.85 \times 10^{-3}\alpha L \\
 & - 0.05\alpha\mu - 3.05 \times 10^{-3}\alpha V + 0.097L\mu + 3.75 \times 10^{-3}LV - 0.06\mu V \\
 & + 0.034\alpha^2 + +0.058L^2 - 9.65\mu^2 - 0.01V^2
 \end{aligned}
 \tag{6}$$

#### 4.2.2. Is the developed model adequate?

The adequacy of the experiential relationship has been checked by using ANOVA and the results are shown in 4-7 tables. In the current study, the significance of the experiential relationship has been checked by considering F and probability values. Also, the influence of each factor on the responses has been assessed by using F-values. The sufficiency of fit for the model has been shown by the value of (R2 > 0.99). Good correlation can be seen between the anticipated and adjusted R2. Tables 4-7 show the value of probability > F for the experiential relationship which is less than 0.05. As can be seen, lack of fit was not significant for the model [11].

Table 4. ANOVA for drawing force.

Source	Sum of Squares	Degree of Freedom	Means of Square	F-Value	Prob>F	Significance
Model	6.64×10 <sup>8</sup>	14	4.74×10 <sup>7</sup>	340.85	<0.0001	Significant
α	2.49×10 <sup>8</sup>	1	2.49×10 <sup>8</sup>	1788.58	<0.0001	
L	1.78×10 <sup>6</sup>	1	1.78×10 <sup>6</sup>	12.83	0.0027	
μ	3.25×10 <sup>8</sup>	1	3.25×10 <sup>8</sup>	2336.81	<0.0001	
V	8.42	1	8.42	6.04×10 <sup>-5</sup>	0.9939	
αL	423.3	1	423.3	3.041×10 <sup>-3</sup>	0.9567	
αμ	5.86×10 <sup>7</sup>	1	5.86×10 <sup>7</sup>	421.1	<0.0001	
αV	529.69	1	529.69	3.8×10 <sup>-3</sup>	0.9516	
Lμ	5.95×10 <sup>5</sup>	1	5.95×10 <sup>5</sup>	4.28	0.0562	
LV	6517.3	1	6517.3	0.047	0.8316	
μV	120.45	1	120.45	8.65×10 <sup>-4</sup>	0.9769	
α <sup>2</sup>	1.05×10 <sup>5</sup>	1	1.05×10 <sup>5</sup>	75.61	<0.0001	
L <sup>2</sup>	17.47	1	17.47	1.255×10 <sup>-4</sup>	0.9912	
μ <sup>2</sup>	1234.36	1	1234.36	8.86×10 <sup>-3</sup>	0.9262	
V <sup>2</sup>	3491.19	1	3491.19	0.025	0.8763	
Residual	2.08×10 <sup>6</sup>	15	1.39×10 <sup>5</sup>	-	-	Insignificant
Lack-of-fit	2.08×10 <sup>6</sup>	10	2.08×10 <sup>5</sup>	3.57	0.8652	
$R^2=0.9969$		$R^2_{adjusted}=0.9939$		$R^2_{predicted}=0.9864$		



Table 5. ANOVA for linear thickness distribution.

Source	Sum of Squares	Degree of Freedom	Means of Square	F-Value	Prob>F	Significance
Model	0.69	14	0.049	12.25	<0.0001	Significant
$\alpha$	$5.064 \times 10^{-3}$	1	$5.064 \times 10^{-3}$	1.26	0.2790	
$L$	$6.45 \times 10^{-3}$	1	$6.45 \times 10^{-3}$	1.61	0.2233	
$\mu$	$4.72 \times 10^{-3}$	1	$4.72 \times 10^{-3}$	1.18	0.2944	
$V$	$4.48 \times 10^{-3}$	1	$4.48 \times 10^{-3}$	1.12	0.3062	
$aL$	$3.86 \times 10^{-3}$	1	$3.86 \times 10^{-3}$	0.96	0.3415	
$a\mu$	$4.76 \times 10^{-3}$	1	$4.76 \times 10^{-3}$	1.19	0.2924	
$aV$	$5.6 \times 10^{-3}$	1	$5.6 \times 10^{-3}$	1.4	0.2550	
$L\mu$	$4.13 \times 10^{-3}$	1	$4.13 \times 10^{-3}$	1.03	0.3257	
$LV$	$4.98 \times 10^{-3}$	1	$4.98 \times 10^{-3}$	1.24	0.2821	
$\mu V$	$5.06 \times 10^{-3}$	1	$5.06 \times 10^{-3}$	1.27	0.2783	
$\alpha^2$	0.14	1	0.14	34.36	<0.0001	
$L^2$	0.15	1	0.15	38	<0.0001	
$\mu^2$	0.027	1	0.027	6.68	0.0207	
$V^2$	0.028	1	0.028	6.97	0.0185	
Residual	0.06	15	$4 \times 10^{-3}$	-	-	
Lack-of-fit	0.06	10	$6 \times 10^{-3}$	0.074	0.1119	Insignificant
$R^2=0.9915$		$R^2_{adjusted}=0.9445$		$R^2_{predicted}=0.9637$		

Table 6. ANOVA for peripheral thickness distribution.

Source	Sum of Squares	Degree of Freedom	Means of Square	F-Value	Prob>F	Significance
Model	0.67	14	0.048	12.24	<0.0001	Significant
$\alpha$	0.018	1	0.018	4.6	0.0487	
$L$	$6.99 \times 10^{-3}$	1	$6.99 \times 10^{-3}$	1.78	0.2015	
$\mu$	$3.25 \times 10^{-3}$	1	$3.25 \times 10^{-3}$	0.83	0.3769	
$V$	$5.07 \times 10^{-3}$	1	$5.07 \times 10^{-3}$	1.29	0.2733	
$aL$	0.014	1	0.014	3.49	0.0812	
$a\mu$	$3.45 \times 10^{-3}$	1	$3.45 \times 10^{-3}$	0.88	0.3625	
$aV$	$5.35 \times 10^{-3}$	1	$5.35 \times 10^{-3}$	1.49	0.2414	
$L\mu$	$6.058 \times 10^{-3}$	1	$6.058 \times 10^{-3}$	1.55	0.2330	
$LV$	$5.62 \times 10^{-3}$	1	$5.62 \times 10^{-3}$	1.43	0.2496	
$\mu V$	$4.62 \times 10^{-3}$	1	$4.62 \times 10^{-3}$	1.18	0.2946	
$\alpha^2$	0.12	1	0.12	30.58	<0.0001	
$L^2$	0.14	1	0.14	36.32	<0.0001	
$\mu^2$	0.024	1	0.024	6.16	0.0254	
$V^2$	0.021	1	0.021	5.25	0.0369	
Residual	0.059	15	$3.92 \times 10^{-3}$	-	-	
Lack-of-fit	0.059	10	$5.88 \times 10^{-3}$	0.085	0.2439	Insignificant
$R^2=0.9932$		$R^2_{adjusted}=0.9425$		$R^2_{predicted}=0.9648$		

Table 7. ANOVA for mean square error.

Source	Sum of Squares	Degree of Freedom	Means of square	F-Value	Prob>F	Significance
Model	0.25	14	0.018	43.66	<0.0001	Significant
$\alpha$	0.07	1	0.070	169.99	<0.0001	
$L$	$6.57 \times 10^{-3}$	1	$6.57 \times 10^{-3}$	16	0.0012	
$\mu$	0.13	1	0.13	328	<0.0001	
$V$	$1.2 \times 10^{-3}$	1	$1.2 \times 10^{-3}$	2.93	0.1076	
$aL$	$4.64 \times 10^{-3}$	1	$4.64 \times 10^{-3}$	11.3	0.0043	
$a\mu$	0.013	1	0.013	30.58	<0.0001	
$aV$	$5.04 \times 10^{-4}$	1	$5.04 \times 10^{-4}$	1.23	0.2856	
$L\mu$	$5.32 \times 10^{-5}$	1	$5.32 \times 10^{-5}$	0.13	0.7238	
$LV$	$2.54 \times 10^{-4}$	1	$2.54 \times 10^{-4}$	0.62	0.4437	
$\mu V$	$2.098 \times 10^{-3}$	1	$2.098 \times 10^{-3}$	5.1	0.0392	
$\alpha^2$	$8.73 \times 10^{-3}$	1	$8.73 \times 10^{-3}$	20.36	0.0004	
$L^2$	$7.45 \times 10^{-5}$	1	$7.45 \times 10^{-5}$	0.18	0.6763	
$\mu^2$	$3.81 \times 10^{-5}$	1	$3.81 \times 10^{-5}$	0.093	0.7648	
$V^2$	$1.36 \times 10^{-4}$	1	$1.36 \times 10^{-4}$	0.33	0.5727	
Residual	$6.16 \times 10^{-3}$	15	$4.11 \times 10^{-4}$	-	-	
Lack-of-fit	$6.16 \times 10^{-3}$	10	$6.165 \times 10^{-4}$	0.091	0.4891	Insignificant
$R^2=0.9976$		$R^2_{adjusted}=0.9537$		$R^2_{predicted}=0.9529$		

### 5. Optimization Process

#### 5.1. Utilizing PCA to find a suitable weight factor for each response

In optimization process, the weight of each factor should be determined according to importance and in the current research principal component analysis (PCA) has been used to reach this goal. It is worth notifying that PCA is a series of statistical analyses which are employed to observe the importance of the quality of each character. Information overlap and internal correlation occur in multivariate research due to the number of variables. In these cases, PCA could be useful to address this issue by reducing the dimension to detect uncorrelated factors. More information about the PCA is found in references [10, 11]. In table 8 the evaluation of the correction coefficient matrix and characterization of the corresponding values have been shown. The eigenvector corresponding to each eigenvalue is listed in Table 9. Table 10 illustrates the contributions of DF, LTD, PTD and MSE which are 0.2287, 0.2841, 0.2501 and 0.2372, respectively.

Table 8. Eigenvalues and explained variations for principal component.

Principal component	Eigenvalues	Explained variations (%)
First	0.0061	0.15
Second	0.0488	1.22
Third	1.6975	42.43
Fourth	2.2476	56.19

Table 9. Eigenvectors for principal component.

Quality characteristics	Eigenvectors			
	first principal component	second principal component	third principal component	fourth principal component
DF	-0.203	-0.7064	-0.5215	-0.4782
LTD	-0.7105	-0.011	-0.4595	0.5330
PTD	-0.7025	-0.0149	0.5061	-0.5001
MSE	0.0362	-0.7077	0.5106	0.4870

Table 10. The contribution of each individual quality characteristic for the fourth principal component.

Quality characteristics	Contribution
DF	0.2287
LTD	0.2841
PTD	0.2501
MSE	0.2372

#### 5.2. Creation of objective function

Multi-criteria problem has been converted to a single criterion task due to multi-objective optimization approach. Equation (6) shows the objective function.

$$F = +w_1 \hat{DF} - w_2 \hat{LTD} - w_3 \hat{PTD} + w_4 \hat{MSE} \tag{6}$$

Where w1, w2, w3 and w4 are the weighting factors that are related to each output which was obtained through principal component analysis.

DF , LTD , PTD and MSE are the normalized values of DF, LTD, PTD and MSE that were achieved by the following equations:

$$\hat{DF} = \frac{DF - DF_{min}}{DF_{max} - DF_{min}} \tag{7}$$

$$\hat{LTD} = \frac{LTD - LTD_{min}}{LTD_{max} - LTD_{min}} \tag{8}$$

$$\hat{PTD} = \frac{PTD - PTD_{min}}{PTD_{max} - PTD_{min}} \tag{9}$$

$$\hat{MSE} = \frac{MSE - MSE_{\min}}{MSE_{\max} - MSE_{\min}} \quad (10)$$

I should hasten to add that, "min" and "max" are signs of minimum and maximum values of given parameters, indexless term is the quality characteristic which has been obtained from RSM. Simulated annealing algorithm is used for minimization aims, which is the key reason that LTD and PTD were shown by a minus sig. The constructed objective function (i.e. Eq. (6)) is associated with simulated annealing algorithm and optimization is performed.

### 5.3. Utilizing SA to find the optimal combination and results validation

The flowchart of SA and its procedure, shown in Fig. 6, are aimed to reach the optimal solution. Same as the other evolutionary algorithms, SA requires its own parameters which should be carried out. The requirement for carrying SA algorithm has been shown in Table 11.

MATLAB software has been used for developing SA code but prior to utilizing this code, it had been checked by some optimization's function, namely Rastrigin and Rosenbrock, the results have shown that the results are able to discover the optimal results with high accuracy.

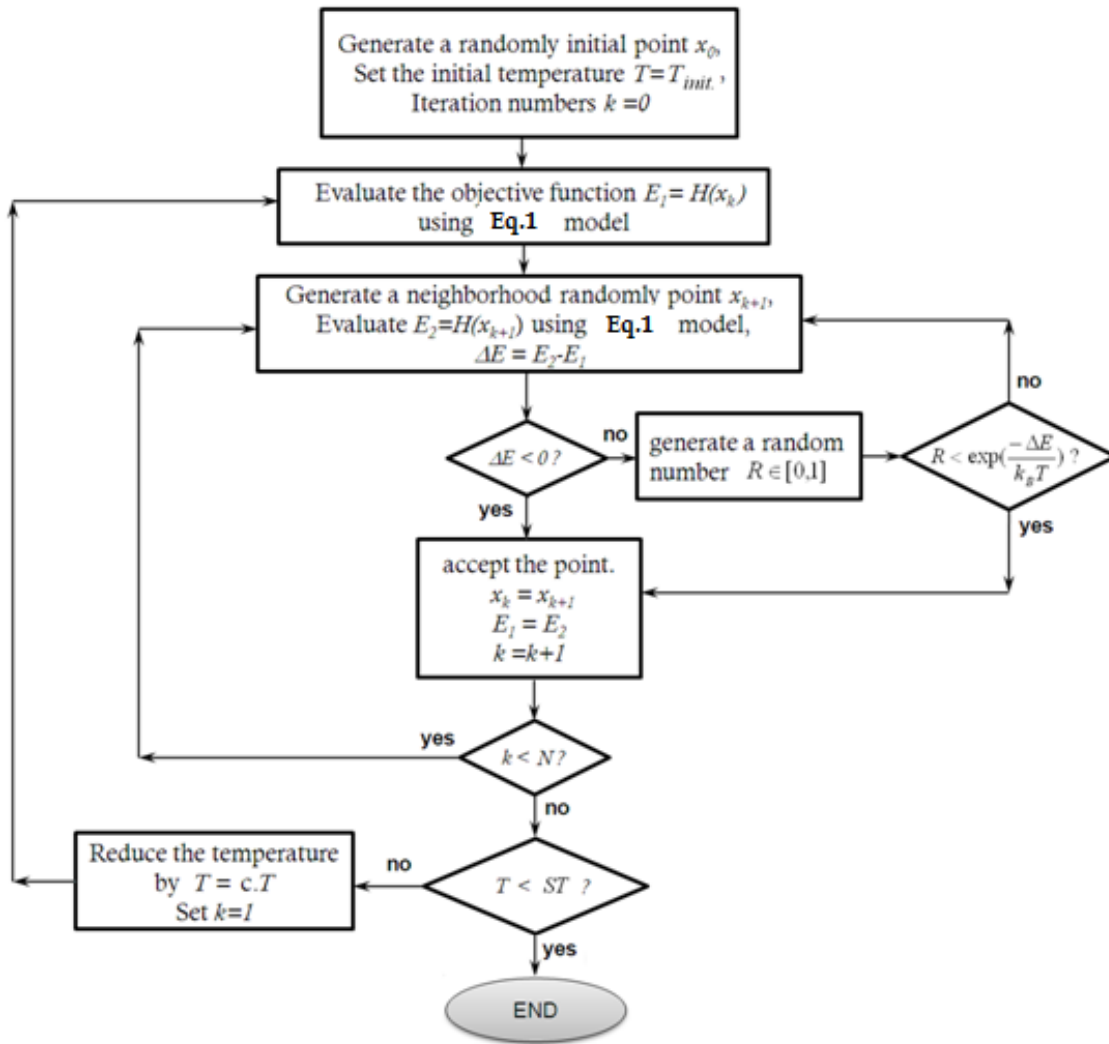


Fig. 6. Simulated annealing approach [13].

Table 11. SA'S setup parameters [12].

Parameter	Value/function	Remark
$X_0$	[0 0 0 0]	Initial point
$T_{init}$	500	Initial temperature
$H(X)$	Eq. 6	Objective function which uses normalized RSM models along with their related weight factors
R	$X=rand(4,1)$	Random vector $X$ in the range of [0,1]
$k_B$	1	Boltzmann constant
ST	10e-8	Stop temperature
C	0.9	Cooling rate
N	300	Maximum number of tries within one temperature

The optimal solution which has been achieved through simulated annealing has been shown in Table 12. Ten runs have been done to check the accuracy of the algorithm. Afterward, experimental and numerical runs have been carried out by considering the optimal combination. The results show the comparison of experimental, FE and RSM-SA in Table 13. It can be seen that there is adequate correlation, 95% for FE and 90% for experimental, between the confirmatory tests. Eventually, it is argued that the offered method has accuracy and could be used in tube sinking's optimization. Also, it could be utilized in the other manufacturing process to swell the number of experiments and cost.

Table 12. Optimal parameter combination achieved from simulated annealing.

$\alpha$ (deg)	$\mu$	V (mm/min)	L (mm)	DF (N)	LTD (mm)	PTD (mm)	MSE
7.49	0.28	5.01	3.03	10112.13	1.09	1.1	0.3184

Table 13. Experimental, FE and RSM-SA optimal results comparison.

Characteristic	RSM-SA	FE simulation	Experiment
Drawing force (N)	10112.13	9667.2	9384.057
Linear thickness (mm)	1.09	1.046	1.0148
Peripheral thickness (mm)	1.1	1.064	1.0318
Mean square error	0.3184	0.3032	0.02997

## 6. Conclusion

In this present work, an integrated approach including numerical, statistical and evolutionary techniques was proposed for the optimization of tube sinking process in fabricating square sections from round tubes. Firstly, ABAQUS/EXPLICIT software has been employed to develop the tube sinking of pure copper. In the next step, FE results have been validated with experimental results. Afterward, a series of runs, 25 FE run, have been implemented based on CCD design matrix to achieve the data to develop RSM models. Adequacies of MSE, drawing force linear and peripheral thickness distribution were performed by analyzing the variances, and the high R2 value implied that the RSM models have sufficient correlation between experimental and numerical results. Combination of FE model and RSM could be useful in predicting the tube sinking process. In addition, this combination has reduced the number of experimental tests which are really time-consuming processes. Next, appropriate weight factor has been analyzed by using PCA for constructing objective function. In the last step, the optimum parameters have been found by using RSM-SA. Optimization process aimed to minimize the drawing force and MSE and maximize the linear and peripheral thickness distribution. The combination of die angle of 7.5 deg, friction coefficient of 0.3, entrance velocity of 5 mm/min and bearing length of 3 mm is the desirable result which could be achieved. This optimal combination has been confirmed through one additional run and another experimental test. According to what has been found in the current research, it can be mentioned that the combination of RSM and SA is an effective method to model and optimize the tube sinking process.

## 7. References

- [1] L.S. Bayoumi, A.S. Attia, Determination of the forming tool load in plastic shaping of a round tube into a square tubular section. *J Mater Process Technol* 209(2009) 1835-1842.
- [2] L.S. Bayoumi, Cold drawing of regular polygonal tubular sections from round tubes, *Int J Mech Sci* 43(2001) 241-253.
- [3] Y.M. Hwang, Y. Altan Finite element analysis of tube hydroforming processes in a rectangular die, *Fini Ele in Analys Des* 39(2002)1071-1082.
- [4] K. Manabe, M. Amino, Effects of process parameters and material properties on deformation process in tube hydroforming. *J Mater Process Technol* 123(2002) 285-291.
- [5] G.T. Kridli, L. Bao, P.K. Malliek, Y. Tian, Investigation of thickness variation and corner filling in tube hydroforming, *J Mater Process Technol* 133(2003) 287-296.
- [6] R. Bihanta, Q.H. Bui, M. Guillot, G. D'Amours, A. Rahem, M. Fafard, A new method for production of variable thickness aluminium tubes: Numerical and experimental studies, *Journal of Materials Processing Technology* 211(2011) 578–589.
- [7] D.K. Leu, J.Y. Wu, Finite element simulation of the squaring of circular tube, *Int J Adv Manuf Technol* 25(2005) 691-699.
- [8] F.O. Neves, T. Buttons, C. Caminaga, F.C. Gentile, Numerical and experimental analysis of tube drawing with fixed plug (2005).
- [9] P. Karnezis, D.C.J. Farrugia, Study of cold tube drawing by finite-element modeling, *Journal of Materials Processing Technology* 80(1998) 690–694.
- [10] K. Yoshida, H. Furuya, Mandrel drawing and plug drawing of shape-memory-alloy fine tubes used in catheters and stents, *Journal of Materials Processing Technology*, 153(2004) 145–150.
- [11] M. Ghasemi-Baboly, M. Aminian, Z. Leseman, R. Teimouri, Application of soft computing techniques in modeling and analysis of MRR and Taper in laser machining process as well as weld strength and weld width in laser welding process. *Soft Comput*, DOI 10.1007/S00500-014-1305-x, (2104).
- [12] Vazini Shayan, R. Azar Afza, R. Teimouri, Parametric study along with selection of optimal solutions in dry wire cut machining of cemented tungsten carbide (WC-Co). *J Manuf Proc* 15(2013) 644-658.
- [13] S. Parsa Khanghah, M. Bouzarpoor, M. Lotfi, R. Teimouri, Optimization of micro-milling parameters regarding burr size minimization via RSM and simulated annealing algorithm. *Transaction of the Indian Institute of Metal*, DOI 10.1007/s12666-015-0525-9.
- [14] H. Sohrabpoor, S. Parsa Khanghah, R. Teimouri. Investigation of lubricant condition and machining parameters while turning of AISI 4340. *Int J Adv Manuf Technol*. DOI 1 0.1007/s00170-014-6395-1, (2105).
- [15] Y. Rostamiyan, A. Seidnalo, H. Sohrabpoor, R. Teimouri, Experimental studies on ultrasonically assisted friction stir spot welding of AA6061. *Arch Civil Mech Eng*. DOI: 10.1016/j.acme.2014.06.005.
- [16] M. Ahmadnia, A. Seidanloo, R. Teimouri, Y. Rostamiyan, K.H. Tirtashi, Determining influence of ultrasonic assisted friction stir welding parameters on mechanical and tribological properties of AA6061 joints. *Int J Adv Manuf Technol*. DOI 1 0.1007/s00170-015-6784-0, (2015).
- [17] M. Hosseinzadeh, M. Ghasempour Mouziraji, An analysis of tube drawing process used to produce squared sections from round tubes through FE simulation and response surface methodology, *The International Journal of Advanced Manufacturing Technology* 87.5-8 (2016) 2179-2194.
- [18] M. Salehi, M. Hosseinzadeh, M. Elyasi, A study on optimal design of process parameters in tube drawing process of rectangular parts by combining box–behnken design of experiment, response surface methodology and artificial bee colony algorithm, *Transactions of the Indian Institute of Metals* 69.6 (2016) 1223-1235.
- [19] Jafari, M., Lotfi, M., Ghaseminejad, P., Roodi, M., Teimouri, R. (2015). Numerical control and optimization of springback in L-bending of magnesium alloy through FE analysis and artificial intelligence. *Transactions of the Indian Institute of Metals*, 68(5), 969-979.

## رویکرد ترکیبی مبتنی بر آنالیز عددی، آماری و روش هوشمند جهت بهینه سازی فرآیند کشش لوله در تولید لوله با مقطع مربعی از مقطع دایروی

مهران قاسمپور موزیرجی<sup>1\*</sup>، مرتضی حسین زاده<sup>2</sup>، محمد بخشی<sup>3</sup>، جمال مکتوبیان<sup>4</sup>

<sup>1</sup>کارشناس ارشد مکانیک، دانشکده مهندسی، دانشگاه آزاد اسلامی واحد ساری، ایران.

<sup>2</sup>استادیار، دانشکده مهندسی، دانشگاه آزاد اسلامی واحد آیت الله آملی، ایران.

<sup>3</sup>استاد، دانشکده مهندسی مکانیک، دانشگاه صنعتی نوشیروانی بابل، ایران.

<sup>4</sup>کارشناس ارشد فناوری اطلاعات، دانشکده مدیریت اطلاعات و سیستم ها، دانشگاه میسور، هند.

**چکیده:** در فرایند کشش لوله پارامترهای زیادی نقش دارند. بنابراین یافتن پارامترهای بهینه میتواند موضوع مهمی باشد. در پژوهش حاضر کشش لوله تو خالی جهت تولید لوله های مربعی مورد بررسی قرار گرفته است. جهت انجام شبیه سازی از روش اجزای محدود استفاده شده است. جهت یافتن پارامترهای بهینه از شبیه سازی اجزای محدود و روش پاسخ سطح و تبرید شبیه سازی شده استفاده شده است. هدف از انجام پروژه دستیابی به بالاترین توزیع ضخامت و کمترین نیروی کشش میباشد که اختصاص وزن مناسب بدست آمده است. نتایج بدست آمده از بهینه سازی دارای تطابق مناسبی با نتایج شبیه سازی و آزمون تجربی داشته اند.

**واژه های کلیدی:** کشش لوله تو خالی، مقطع مربعی، بهینه سازی چند هدفه